Fine-Structure Transition in Ne($^3P_0$) on Ne($^1S_0$) Collisions at Thermal Energies

I. Colomb de Daunant, G. Vassilev, M. Dumont, and J. Baudon
Laboratoire de Physique des Lasers, Université Paris-Nord, F-93430 Villetaneuse, France
(Received 15 December 1980)

The collision-induced exothermic fine-structure transition Ne($^3P_0$)-Ne($^3P_2$) has been observed in a crossed-effusive-beam experiment, by measuring the time of flight of metastable atoms scattered perpendicularly to the incident-beam plane. In this direction, the elastic scattering is kinematically discriminated. The identification of the transition is achieved by pumping $^3P_0$ or $^3P_2$ levels with a cw dye laser.

PACS numbers: 32.30.Bv, 34.50.-s

Collision-induced fine-structure transitions have been widely investigated experimentally since the 1960's especially for excited alkali-alkali (or rare-gas) atom systems. Recent progress has been made in this field, in velocity-selected crossed-beam or beam-cell experiments.[1] From the theoretical point of view, the collision problem itself may be considered as solved in principle[2] and the main remaining problem is to determine the molecular energies and the couplings between molecular states. For excited alkali–rare-gas (or even alkali) systems this determination is generally greatly simplified by the fact that they can be considered approximately as one-electron systems. This allows the use of pseudopotential or model-potential methods,[3] instead of heavy *ab initio* calculations.

On the other hand, fine-structure transitions in metastable-rare-gas-atom (R^*)–rare-gas-atom (R') collisions have not been so widely studied. A low-pressure discharge is generally used to produce metastable atoms in a cell and collision processes are investigated by optical techniques.[4] In swarm experiments, the rate coefficients of some inelastic processes have been determined for particular velocity distributions.[5] Crossed-beam experiments have been also performed with metastable rare-gas atoms as projectile, but they have been essentially devoted to the study of the elastic scattering,[6] or the Penning ionization.[7] $(RR')^*$ is a one-electron–plus–one-hole system and consequently, it is more complex than alkali–rare-gas systems. In spite of that, more or less simplified models or elaborated *ab initio* methods[8] have been proposed to determine the potential energies. Comparisons between theoretical predictions and experimental results (elastic scattering, optical properties of excimers, etc.) are generally concerned with the potential curves themselves, rather than with the couplings between different molecular states. On the other hand, fine-structure transition processes at thermal energies are very sensitive to potential shapes and to dynamical or spin-orbit couplings at intermediate and large internuclear distances ($\gtrsim$ few atomic units). In this paper an original experimental method to study exothermic inelastic ("superelastic") processes is presented. It has been applied to the fine-structure transition

$$\mathrm{Ne}^*(2p^5 3s\ ^3P_0) + \mathrm{Ne}(2p^6\ ^1S_0) \rightarrow \mathrm{Ne}^*(2p^5 3s\ ^3P_2) + \mathrm{Ne}(2p^6\ ^1S_0) + Q$$

($Q = 96$ meV), which has already been investigated theoretically by Cohen, Collins, and Lane.[9]

The experimental setup has been described elsewhere[10] and only its main features are reported here (Fig. 1). Two effusive beams of neon cross at right angle. One of them is chopped mechanically (10-μs-wide pulses, separated by 840 μs). Delayed $^3P_0$ and $^3P_2$ metastable atom pulses (10 to 20 μs wide) are produced by electronic bombardment of the second beam. Metastable atoms scattered in a given direction are detected by a channel-electron multiplier. Their time-of-flight (TOF) spectrum is finally given by a multichannel analyzer started by the electron-

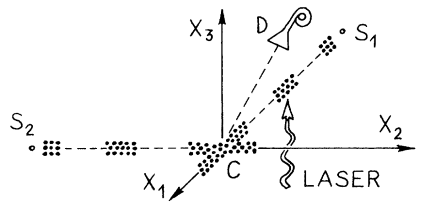

FIG. 1. Experimental arrangement: Ground-state atom pulses are emitted at point S_2, in the x_2 direction. Delayed metastable atom pulses are emitted at S_1, in the x_1 direction. Scattered metastable atoms are detected by a channel electron multiplier D. ($\overline{S_1C}$ = 110 mm, $\overline{S_2C}$ = 15 mm, $\overline{CD}$ = 70 mm).

gun voltage pulses. The synchronized chopping of the two beams, combined with the TOF measurement, provides a velocity selection in both beams: For a given elastic or exothermic collision process, each TOF in a given scattering direction is related unequivocally to a pair of initial velocities (v_1 of the metastable atom, v_2 of the ground-state atom). In the present energy range (30–120 meV), the only energetically accessible processes which produce metastable (i.e., detectable) atoms are the elastic scattering and the fine-structure transitions $^3P_0 \rightleftharpoons {}^3P_2 + 96$ meV. The $J=2 \rightarrow J=0$ transition probability is weak since its energy threshold is higher than the most probable relative energy (78 meV). On the other hand, the $J=0 \rightarrow J=2$ transition can be considered *a priori* as observable. When the scattering direction lies in the x_1-x_2 plane, the inelastic TOF spectrum has its maximum rather close to that of the elastic one (at 261 and 290 μs for $\theta_{1ab}=15°$). Because of the widths of the spectra, it is difficult to separate the contributions of the two processes, especially when the probability of the inelastic one is small. The observation of the superelastic process requires the use of either two monoenergetic atomic beams, or some experimental trick to better separate the two TOF spectra from each other. From this latter point of view, the detection of the scattered metastable atoms in the direction Cx_3 perpendicular to the initial velocity plane offers some interesting properties: (i) As it is seen on the Newton velocity diagram (Fig. 2), the final velocity v_1' of the elastically scattered metastable atoms is zero and the elastic contribution to the TOF spectrum vanishes. (ii) The final velocity v_1'' of the scattered atom after a superelastic collision is entirely determined by the internal energy variation Q: $v_1''=(Q/2\mu)^{1/2} \approx 680$ m/s, where μ is the reduced mass. In other words, when two beams containing atoms or molecules of equal mass, with arbitrarily wide velocity distributions, cross at right angle, any superelastic process produces a monoenergetic beam in the perpendicular direction. It may be noticed that the c.m. scattering angle corresponding to the direction x_3 is $\theta=90°$ for equal incident velocities. (iii) This technique could be generalized to systems with a different mass: When the metastable particle is the heaviest one ($\gamma=m_1/m_2>1$), no elastically scattered particle is detected in the x_3 direction; however, the inelastically scattered beam, at $\alpha=0$, is no longer monokinetic, but v_1'' depends only on v_1:

$$v_1''=(1+\gamma)^{-1/2}[(2Q/m_1)+(1-\gamma)v_1^2]^{1/2}.$$

The shift and the broadening of the peak are then proportional to $(1-\gamma)$. Because of mechanical constraints, it has not been possible to put the detector exactly in the x_3 direction. The investigated scattering direction lies in the x_2-x_3 plane and it makes an angle α ($10° \leq \alpha \leq 26°$) with the x_3 axis. In such conditions, the final velocities are

$$v_1'(\alpha)=v_2\sin\alpha,$$

$$v_1''(\alpha)=\tfrac{1}{2}\{[4v_1''(0)^2+v_2^2\sin^2\alpha]^{1/2}+v_2\sin\alpha\},$$

respectively, for the elastic and the superelastic process. The scattering direction solid angle viewed by the detector has a half apex angle of 4°. In the observed TOF spectra at $\alpha=10°$, 18°, 20°, and 26° shown in Fig. 3, inelastic and elastic contributions are seen.[11] When α decreases, the first one remains at almost the same place, whereas the second is shifted toward large TOF and becomes broader and smaller relative to the first one. The broken curves are TOF spectra calculated (in arbitrary units) by using the actual velocity distributions of the two beams with the following assumptions: zero angular spread, infinite resolution of the TOF measurement, and equal and velocity independent elastic and inelastic cross sections. The ratio of the c.m. solid angles ($\Delta\omega_{el}/\Delta\omega_{inel} \approx 3.84 \sin\alpha$) is not taken into account in this calculation; it makes the experimental elastic peak decrease faster

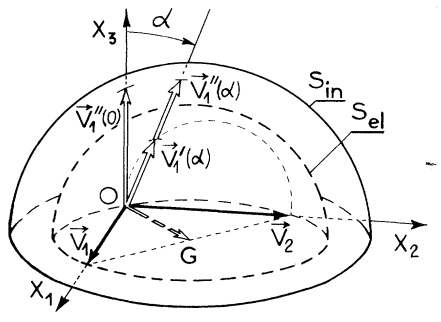

FIG. 2. Newton diagram: $\vec{v}_{1,2}$ are, respectively, the initial velocities of the metastable and the ground-state atoms. The final velocity $\vec{v}_1'$ of an elastically scattered metastable atom is given by the intersection of the sphere S_{el} radius $[r=\frac{1}{2}(v_1^2+v_2^2)^{1/2}]$ by the scattering direction; the inelastic velocity $\vec{v}_1''$ is obtained in the same way, with S_{in} radius $[r'=(r^2+Q/2\mu)^{1/2}]$.

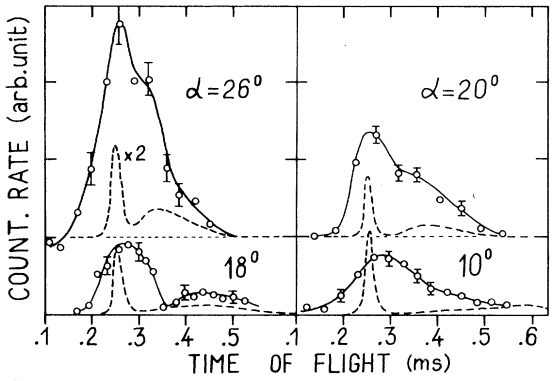

FIG. 3. Full line: TOF spectra observed at a small angle α with respect to the x_3 direction. Broken line: calculated spectra (see text).

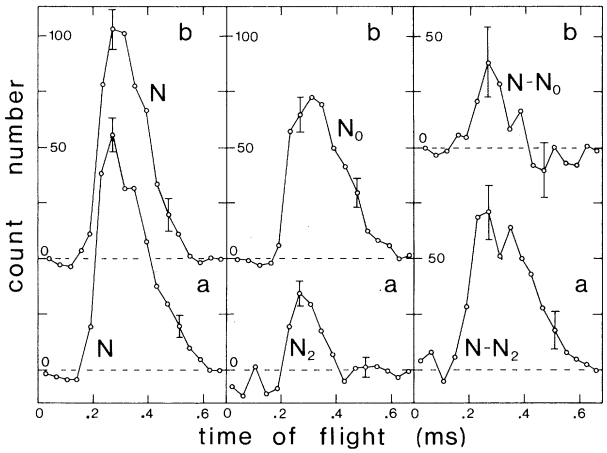

FIG. 4. TOF spectra observed at $\alpha = 20°$. (a) N, without laser; N_2, the $^3P_2$ level is pumped ($\lambda = 6143$ Å). This spectrum represents the Ne($^3P_0$) + Ne($^1S_0$) scattering, in which the superelastic process dominates (relatively narrow peak centered on $t \approx 280\ \mu$s). (b) N, without laser; N_0, the $^3P_0$ level is pumped ($\lambda = 6163$ Å). Only the $^3P_2$ elastic scattering persists (broader peak centered on $t \approx 360\ \mu$s). N_0 is recovered in $N - N_2$, and N_2 in $N - N_0$, apart from a small (negative) contribution due to the radiative feedback to the $^3P_2$ level. Typical statistical error bars are shown. Each experimental run takes about two hours.

than the calculated one when α approaches zero.

In order to confirm the existence of the collision-induced $^3P_0 \rightarrow {}^3P_2$ transition and to get an estimate of its probability with respect to the elastic process at $\theta \approx 90°$ ($\alpha = 20°$), we have used a cw dye laser to destroy—at least partly—the population of one or the other level in the incident metastable atom beam, before the collision. The dye-laser frequency is stabilized by means of a Fabry-Pérot interferometer (stability ~1 MHz), and locked to the chosen neon line by means of a saturated absorption Ne cell.[12] The light beam crosses the metastable atom beam at right angle, 1 cm before the collision point. In order to improve the efficiency of the optical pumping, the laser beam crosses twice the atomic beam and its convergence has been matched to the slight divergence of the atomic beam (~1.5°). Finally the optical transitions can be saturated with a moderate laser power ($\gtrsim$20 mW). Preliminary TOF measurements on the incident metastable beam have shown that the effect of the laser [$1s_5(^3P_2) - 2p^6$, $\lambda = 6143$ Å and $1s_3(^3P_0) - 2p_2$, $\lambda = 6163$ Å] is to reduce the metastable intensity without any appreciable change in the velocity distribution. The 6143-Å line causes a decrease of about 75% of the intensity. In saturation conditions, the remaining $^3P_2$ population should be zero. As a $J = 2 \rightarrow J = 2$ transition is used, no radiative feedback to the $^3P_0$ level is expected. The 6163-Å line reduces the intensity by about 10%. Because the upper level of the transition ($J = 1$) partly decays to the $^3P_2$ level (27% in saturation conditions), this means that the $^3P_0$ fraction in the beam is at least 14%. The sum of the two fractions remains smaller than 100%, even if the laser power is increased. This comes probably from an unperfect matching of the two beams. The $^3P_0$ and $^3P_2$ population ratio is close to that of the statistical weights ($\frac{1}{5}$), probably because the metastable atoms are produced by electron bombardment, with an energy ($\approx$60 eV) largely above the thresholds. Many upper levels are excited and they cascade down to the two metastable levels.

The effect of the optical pumping on the TOF spectrum observed at $\alpha = 20°$ is shown in Fig. 4. The elastic and superelastic contributions are now more clearly separated. Taking into account the initial relative populations of $^3P_0$ and $^3P_2$ levels ($\frac{1}{5}$) and the ratio of the c.m. solid angles, one may deduce that the inelastic differential cross section σ_{in} at $\theta \approx 90°$, averaged over the relative velocity, is equal, or even larger than the elastic one, σ_{el}. Previous measurements,[10] normalized to the values calculated by Cohen and Schneider,[13] yield $\sigma_{el} \approx 10 a_0^2/\text{sr}$. The calculated total inelastic cross section Q_{in}[9] is about $10^{-3} a_0^2$ at 100 meV. These values would be consistent if σ_{in} was confined in an extraordinarily narrow angular width (~1.7×10^{-5} rad) around 90°. As this hypothesis is quite unrealistic, it may be

concluded that, in the present energy range, Q_{in} is probably much larger, by a factor of a few 10^3, than the calculated one. In fact, because of the very fast increase of Q_{in} at low energy, this large discrepancy does not imply a dramatic change either in the potential curves or in the couplings. As mentioned in Ref. 9, the $^3P_0 \rightarrow {}^3P_2$ transition is mainly due to the $0_u^- - 0_u^-$ radial coupling at $R_c \approx 6.5$ a.u. If the energy separation at the avoided crossing was smaller (only by a factor of ~1.5) and R_c slightly larger, Q_{in} would be multiplied by the required factor.

[1]R. W. Anderson *et al.*, J. Chem. Phys. 64, 4037 (1976); W. D. Phillips, C. L. Glaser, and D. Kleppner, Phys. Rev. Lett. 38, 1018 (1977); J. Cuvellier *et al.*, J. Phys. B 12, L461 (1979).

[2]F. Masnou-Seuws and R. McCarroll, J. Phys. B 7, 2230 (1974); E. Roueff and J. M. Launay, J. Phys. B 10, L173 (1977).

[3]J. Pascale and J. Vandeplanque, J. Chem. Phys. 60, 2278 (1974); M. Philippe, F. Masnou, and P. Valiron, J. Phys. B 12, 2493 (1979).

[4]C. Bréchignac, R. Vetter, and P. R. Berman, J. Phys. B 10, 3443 (1977).

[5]F. A. Grant and A. D. Krumbein, Phys. Rev. 90, 59 (1953); A. V. Phelps, Phys. Rev. 114, 1011 (1959); P. K. Leichner, J. D. Cook, and S. L. Luerman, Phys. Rev. A 12, 2501 (1975).

[6]B. Brutschy and H. Haberland, Phys. Rev. A 19, 2232 (1979).

[7]A. Pesnelle, G. Watel, and C. Manus, J. Chem. Phys. 62, 3590 (1975).

[8]J. S. Cohen and B. Schneider, J. Chem. Phys. 8, 3230 (1974); F. Spiegelman and J. P. Malrieu, Chem. Phys. Lett. 57, 214 (1978); S. Iwata, Chem. Phys. 37, 251 (1979).

[9]J. S. Cohen, L. A. Collins, and N. F. Lane, Phys. Rev. A 17, 1343 (1978).

[10]I. Colomb de Daunant *et al.*, J. Phys. B 13, 711 (1980).

[11]In these spectra, the background-gas contribution has been subtracted as it is described in Ref. 10.

[12]M. Gorlicki, A. Peuriot, and M. Dumont, J. Phys. (Paris) 41, L275 (1980).

[13]J. S. Cohen and B. Schneider, Phys. Rev. A 11, 884 (1975).